Lack of Interleukin-1 Receptor I (IL-1RI) Protects Mice From High-Fat Diet–Induced Adipose Tissue Inflammation Coincident With Improved Glucose Homeostasis

Fiona C. McGillicuddy,[1] Karen A. Harford,[1] Clare M. Reynolds,[1] Elizabeth Oliver,[1] Mandy Claessens,[1] Kingston H.G. Mills,[2] and Helen M. Roche[1]

OBJECTIVE—High-fat diet (HFD)-induced adipose tissue inflammation is a critical feature of diet-induced insulin resistance (IR); however, the contribution of interleukin-1 receptor I (IL-1RI)-mediated signals to this phenotype has not been defined. We hypothesized that lack of IL-1RI may ameliorate HFD-induced IR by attenuating adipose tissue inflammation.

RESEARCH DESIGN AND METHODS—Glucose homeostasis was monitored in chow- and HFD-fed wild-type (WT) and IL-1RI$^{-/-}$ mice by glucose tolerance and insulin tolerance tests. Macrophage recruitment and cytokine signature of adipose tissue macrophages was evaluated. Insulin sensitivity and cytokine secretion from adipose explants was quantified. Cytokine secretion and adipocyte insulin sensitivity was measured in cocultures of WT or IL-1RI$^{-/-}$ macrophages with 3T3L1 adipocytes. Synergistic effects of IL-1β with tumor necrosis factor (TNF)-α on inflammation was monitored in WT and IL-1RI$^{-/-}$ bone-marrow macrophages and adipose explants.

RESULTS—Lean and obese IL-1RI$^{-/-}$ animals exhibited enhanced glucose homeostasis by glucose tolerance test and insulin tolerance test. M1/M2 macrophage number in adipose tissue was comparable between genotypes; however, TNF-α and IL-6 secretion was lower from IL-1RI$^{-/-}$ adipose tissue macrophages. IL-1RI$^{-/-}$ adipose exhibited enhanced insulin sensitivity, elevated pAKT, lower cytokine secretion, and attenuated induction of phosphorylated signal transducer and activator of transcription 3 and suppressor of cytokine signaling molecule 3 after HFD. Coculture of WT, but not IL-1RI$^{-/-}$ macrophages, with 3T3L1 adipocytes enhanced IL-6 and TNF-α secretion, reduced adiponectin secretion, and impaired adipocyte insulin sensitivity. TNF-α and IL-1β potently synergized to enhance inflammation in WT macrophages and adipose, an effect lost in the absence of IL-1RI.

CONCLUSIONS—Lack of IL-1RI protects against HFD-induced IR coincident with reduced local adipose tissue inflammation, despite equivalent immune cell recruitment. ***Diabetes*** **60:1688–1698, 2011**

From the [1]Nutrigenomics Research Group, University College Dublin Conway Institute, School of Public Health & Population Science, University College Dublin, Dublin, Ireland; and the [2]Immune Regulation Research Group, School of Biochemistry and Immunology, Trinity College Dublin, Dublin, Ireland.

Corresponding author: Helen M. Roche, helen.roche@ucd.ie.

Received 9 September 2010 and accepted 18 March 2011.

DOI: 10.2337/db10-1278

This article contains Supplementary Data online at http://diabetes.diabetesjournals.org/lookup/suppl/doi:10.2337/db10-1278/-/DC1.

F.C.M. and K.A.H. contributed equally to this work.

The emergent pandemic of obesity has demanded greater understanding of associated metabolic complications, including insulin resistance (IR) and type 2 diabetes. Immune cell infiltration into adipose during obesity has been documented with initial infiltration of T cells (1–4) followed by macrophages (5,6). Proinflammatory cytokine release from infiltrating immune cells in turn contributes to a chronic state of inflammation (7), with enhanced local secretion of proinflammatory cytokines, interleukin (IL)-1, IL-6, and tumor necrosis factor (TNF)-α, from the expanding adipose tissue mass (8–11), which in turn induces adipocyte IR in vitro (12–14). Furthermore, abrogation of TNF-α signaling alleviates high-fat diet (HFD)-induced IR in vivo (15), whereas lack of TLR4 protects against free fatty acid–induced IR (16,17). These studies suggest that HFD-induced IR is driven by a pathological immune response; however, the contribution of IL-1 receptor I (IL-1RI) signaling to this phenotype has not yet been deciphered, particularly in the context of adipose tissue biology.

There is much evidence to suggest that IL-1 has a pathogenic role in adipose tissue during obesity. Activation of IL-1β in vivo depends on processing of its pro- to active form by the NLRP3-caspase-1 inflammasome complex (18). Genetic deletion of *NLRP3* (19), or pharmacological inhibition of caspase-1 (20), confer protection against obesity-induced IR, effects potentially attributable to reduced IL-1β. Downstream IL-1 binds to IL-1RI and activates nuclear factor (NF)-κB and Jun NH2-terminal kinase mitogen-activated protein kinase (JNK MAPK) (21,22), which have been implicated in IR (23,24). Furthermore, TNF-α, TLR4, and IL-1 signaling pathways converge at the inhibitor of NFκB kinase (IKK)/NFκB axis (25), with marked protection of IKK$^{-/-}$ mice against IR (26,27). IL-1β also potently induces production of other proinflammatory cytokines, including IL-6. Both IL-1β and IL-6 induce adipocyte IR in vitro (13,14,28), with IL-1β also inhibiting adipogenesis (29). IL-6, via activation of JAK2/STAT3, potently induces expression of suppressor of cytokine signaling molecule (SOCS)-3, which is also associated with IR (30–32). Given this large body of evidence against IL-1, we hypothesized that lack of IL-1RI would protect against HFD-induced adipose inflammation and improve glucose homeostasis.

The current study demonstrates that IL-1RI$^{-/-}$ mice are partially protected from HFD-induced IR but not obesity. The inflammatory profile of IL-1RI$^{-/-}$ adipose explants,

and isolated adipose tissue macrophages (ATMs), was markedly attenuated, coincident with the inability of TNF-α and IL-1β to synergize and augment inflammation in IL-1RI$^{-/-}$ macrophages and adipose. Attenuated inflammation correlated with improved insulin sensitivity in IL-1RI$^{-/-}$ adipose. Furthermore, coculture of IL-1RI$^{-/-}$ macrophages with 3T3L1 adipocytes resulted in a more favorable adipocytokine signature and maintenance of adipocyte insulin sensitivity compared with coculture with wild-type (WT) macrophages. This study demonstrates that inflammatory signals transmitted via IL-1RI are primary mediators of adipose tissue inflammation during obesity.

RESEARCH DESIGN AND METHODS

Materials. Deoxy-D-glucose 2-[1,2-^{3}H(N)]$^-$ was purchased from Perkin-Elmer Analytical Sciences (Dublin, Ireland). Cell culture material was purchased from Lonza (Slough, U.K.). All other reagents unless otherwise stated were from Sigma Aldrich (Dorset, U.K.).

Animals. IL-1RI$^{-/-}$ breeding pairs, on a C57BL/6 background, were purchased from Jackson Laboratories and bred in the University College Dublin for 6–10 generations under specific pathogen-free conditions. Ethical approval was obtained from the University College Dublin Ethics Committee, and mice were maintained according to the regulations of the European Union and the Irish Department of Health. C57BL/6 WT and IL-1RI$^{-/-}$ mice were fed HFD or a nutrient-matched standard-fat chow diet (45% kcal from palm oil and 10% kcal from palm oil, respectively; Research Diets, Brunswick, NJ) starting at age 6 weeks for 12 weeks. Body weight and food intake were recorded weekly. Metabolic tests were performed at baseline (mice aged 6–8 weeks) and after 12 weeks of chow or HFD.

Intraperitoneal glucose and insulin tolerance tests. Mice were fasted for 6 h and were injected intraperitoneally with 25% (wt/vol) glucose (1.5 g/kg; B. Braun Medical, Dublin, Ireland) for glucose tolerance test (GTT) or insulin (0.75 units/kg; Actrapid, Novo Nordisk, Denmark) for insulin tolerance test (ITT), respectively. Glucose levels were monitored at baseline and at indicated time points after the metabolic challenge via tail-vein blood sampling using a blood glucose meter from Accu-Chek (Roche, Dublin, Ireland). Insulin secretory response was monitored in overnight fasted animals, and blood samples were collected at indicated times after glucose load (1.5 g/kg). Insulin levels were measured by enzyme-linked immunosorbent assay (ELISA).

Body mass composition analysis. Body composition (fat, lean, and water content) was analyzed using a Bruker's minispec LF50 body composition analyzer according to the manufacturer's instructions (Bruker Optik, Ettlingen, Germany).

Stromal vascular fraction isolation and purification. Epididymal fat pads were minced, and adipocytes and stromal vascular fractions were separated by collagenase (2 mg/mL) digestion. Stromal vascular cells were filtered, blocked in PBS/2% BSA, and stained with fluorescently labeled antibodies: F4/80-FITC, CD11B-AF647/PE, CD11C-RPE, CD3-APC, CD4-FITC, CD8-PE, or CD117-PE as indicated (AbD Serotec, Kidlington, U.K.). Unstained single stains and fluorescence minus one (FMO) controls were used for setting compensations and gates. Flow cytometry was performed on a Dako CyAn ADP platform (Beckman-Coulter, Clare, Ireland) and analyzed using Summit v4.3 software. In separate studies, F4/80$^+$/CD11B$^+$ cells were isolated from stromal vascular fraction using a BD FACSAria cell sorter (BD Biosciences, Oxfordshire, U.K.).

Ex vivo adipose tissue culture. Adipose tissue from WT and IL-1RI$^{-/-}$ mice was harvested at baseline (aged 6–8 weeks) and after HFD. Adipose explants were placed in 24-well plates (100 mg tissue/well) with 1 mL complete media (Dulbecco's modified Eagle's medium, 10% FBS, and 1% penicillin/streptomycin) for 24 h. Media were harvested, and cytokine secretion (TNF-α, IL-6, and IL-1β) was analyzed by ELISA (Quantikine kits; R&D Systems Europe, Abingdon, U.K.).

Insulin-stimulated glucose uptake transport into adipose tissue explants. Lean and obese adipose explants were placed in 24-well plates (100 mg tissue/well) in PBS + 0.2% BSA before stimulation ± insulin (100 nmol/L) for 15 min. [^{3}H]Glucose (0.1 mmol/L 2-deoxyglucose + 0.5 μCi/mL [^{3}H]deoxyglucose) was added for 45 min. Tissue was washed, lysed in radioimmunoprecipitation assay (RIPA) buffer, and homogenized using a tissue lyser (Qiagen, West Sussex, U.K.). An aliquot of lysate was used for liquid scintillation counting, whereas the remaining aliquot was stored for immunoblot analysis.

Cell culture. 3T3L1 fibroblasts (European Collection of Cell Cultures, Salisbury, U.K.) were differentiated to adipocytes as previously described (33). Bone marrow monocytes, isolated from femurs and tibias of WT and IL-1RI$^{-/-}$ mice, were cultured in Dulbecco's modified Eagle's medium supplemented with 10% FBS, 1% penicillin/streptomycin, and 30% L929 conditioned medium for 7 days to differentiate to the bone marrow macrophage (BMM) phenotype (34). F4/80$^+$/CD11B$^+$ ATMs were seeded (200,000 cells/1 mL media) in 24-well plates and incubated in complete media for 24 h in the absence of any stimulus, and media were harvested for cytokine analysis. NIH-3T3 cells (Panomics, Cambridge, U.K.) stably transfected with a luciferase reporter construct within the NFκB promoter region were maintained in complete media + hygromycin B (100 μg/mL) (Roche, Clare, Ireland).

NIH-3T3 NFκB-luciferase activity assay. Conditioned media from adipose tissue explants were harvested and incubated with NIH-3T3 cells (1×10^5 cells/mL) for 6 h. Cells were washed in PBS and lysed, and luciferase levels were measured by luminescence (Promega, Southampton, U.K.).

IL-1β and TNF-α synergistic studies. NIH-3T3 cells were treated with IL-1β (0.01–10 ng/mL), TNF-α (0.01–10 ng/mL), or IL-1β (0.005–5 ng/mL) and TNF-α (0.005–5 ng/mL) for 6 h, and NFκB-driven luciferase levels were monitored by luminescence. The effect of IL-1β and TNF-α on *1*) IL-6 protein secretion from 3T3L1 adipocytes (24-h treatment); *2*) IL-6, IL-1, SOCS3, and TNF-α mRNA and IL-6 protein secretion from WT and IL-1RI$^{-/-}$ BMMs (24-h treatment); and *3*) IL-6 mRNA and protein secretion in adipose explants (100 mg tissue/mL complete media) (6-h treatment) was monitored.

Coculture study. WT and IL-1RI$^{-/-}$ BMMs were seeded on Corning transwell filters (0.4 μm, Sigma Aldrich) and LPS-stimulated for 30 min. Lipopolysaccharide-containing media was removed, cells were washed in PBS, and fresh media were added. Transwells were transferred to differentiated 3T3L1 adipocytes (day 5 post-differentiation) and left coculture for 5 days. After 72 h, media were harvested for cytokine analysis and fresh media were added. After coculture, insulin-stimulated glucose transport into adipocytes was monitored. On separate identically treated plates, RNA or protein was harvested for further analysis.

In vitro glucose uptake assays. Insulin sensitivity of 3T3L1 adipocytes was monitored in vitro as previously described (35). Briefly, cells were serum starved for 4 h, and glucose was starved in PBS/0.2% BSA for 30 min before insulin (100 nmol/L) stimulation for 15 min. [^{3}H]Deoxyglucose (0.5 μCi/mL cold glucose [0.1 mmol/L]) was added for 30 min before washing with PBS. Cells were lysed in RIPA buffer, and [^{3}H]glucose uptake was measured by liquid scintillation counting. Remaining lysates were stored for immunoblot analysis. Fold increase in glucose uptake over basal (non-insulin–stimulated) is presented.

General laboratory methods. Detailed descriptions of plasma, gene expression, immunohistochemistry, and immunoblot analysis are presented in the Supplementary Data.

Statistical analysis. Data are reported as mean ± SEM. For GTT/ITT studies with multiple time points, we performed two-way repeated-measures ANOVA to test for differences in means between WT and IL-1RI$^{-/-}$ groups. When ANOVA was significant, post hoc Bonferroni corrected *t* tests were applied. Area under the curve analysis was performed on GTT and ITT curves using Graphpad Prism 5 software. For comparison of data between two groups at a single time point, unpaired *t* tests were performed. GraphPad Prism 5 (GraphPad Software, San Diego, CA) was used for statistical analyses. Statistical significance is presented as $^*P < 0.05$, $^{**}P < 0.01$, and $^{***}P < 0.001$ in all figures.

RESULTS

IL-1RI$^{-/-}$ mice exhibit greater glucose tolerance and are partially protected from HFD-induced IR. Glucose homeostasis was markedly improved in IL-1RI$^{-/-}$ compared with WT mice, both at baseline (lean, 6–8 weeks old) and after 12 weeks of HFD by GTT (Fig. 1*A* and *C*) and ITT (Fig. 1*B* and *D*). The GTTs for age-matched chow-fed and HFD-fed IL-1RI$^{-/-}$ mice were equivalent and significantly lower than those for HFD WT mice (Supplementary Fig. 1*A* and *B*). Insulin secretion in response to glucose load was significantly higher in lean IL-1RI$^{-/-}$ mice than in WT mice, despite similar fasting levels (Fig. 1*E*). HFD-fed IL-1RI$^{-/-}$ mice exhibited higher fasting insulin levels compared with WT mice, but had a similar degree of insulin secretion upon glucose load. There was no difference in total body weight between IL-1RI$^{-/-}$ and WT mice at baseline or after HFD (Fig. 1*F*), although epididymal and visceral adipose tissue depot weight was greater in obese IL-1RI$^{-/-}$ animals (Fig. 1*G*). Body mass composition analysis confirmed this increased fat mass (Fig. 1*H*). The

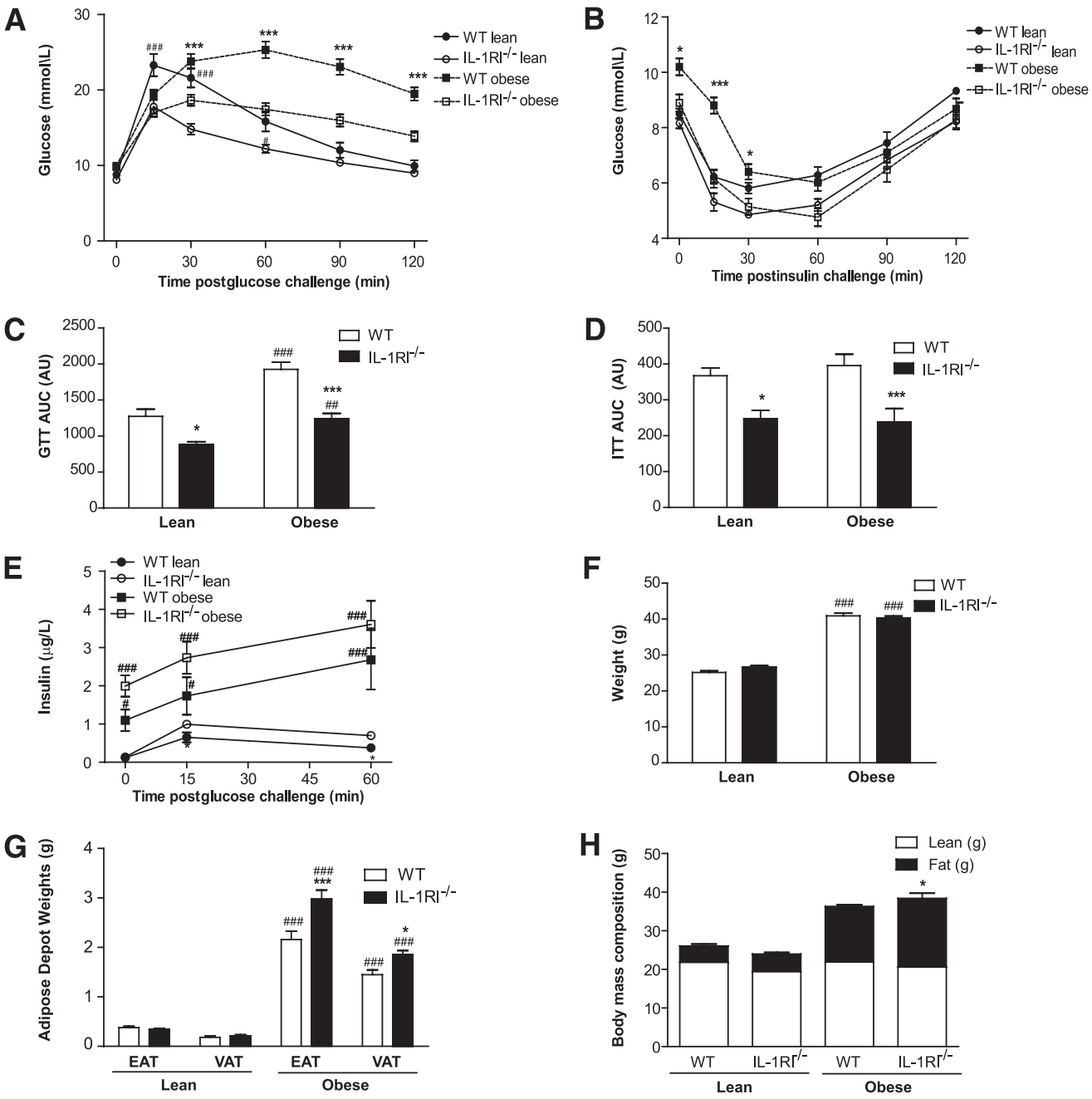

FIG. 1. GTT and ITT in WT and IL-1RI$^{-/-}$ mice at baseline and after HFD. *A*: GTT (1.5 *g*/kg glucose) in 6-h fasted lean and obese WT and IL-1RI$^{-/-}$ animals (●, WT lean; ○, IL-1RI$^{-/-}$ lean; ■, WT obese; □, IL-1RI$^{-/-}$ obese; ***P < 0.001 with respect to [w.r.t.] IL-1RI$^{-/-}$ obese; ###P < 0.001 w.r.t. IL-1RI$^{-/-}$ lean, n = 27–31). *B*: ITT (0.75 units/kg insulin) in 6-h fasted lean and obese WT and IL-1RI$^{-/-}$ animals (●, WT lean; ○, IL-1RI$^{-/-}$ lean; ■, WT obese; □, IL-1RI$^{-/-}$ obese; *P < 0.05, ***P < 0.001 w.r.t. IL-1RI$^{-/-}$ obese, n = 22–31). *C* and *D*: Area under the curve (AUC) for lean and obese animals over course of GTT and ITT was calculated and is expressed as arbitrary units (AU) (*P < 0.5, ***P < 0.001 w.r.t. corresponding WT, ##P < 0.01, ###P < 0.001 w.r.t. corresponding lean, n = 22–31). *E*: Insulin secretion response in overnight fasted lean and obese WT and IL-1RI$^{-/-}$ animals after intraperitoneal injection with 1.5 *g*/kg glucose (*P < 0.05 w.r.t. IL-1RI$^{-/-}$ lean; #P < 0.05, ###P < 0.001 w.r.t. corresponding lean). *F*: Weight of animals at time of metabolic challenge (###P < 0.001 w.r.t. lean, n = 22–31). *G*: Weight of epididymal adipose tissue (EAT) and visceral adipose tissue (VAT) depots of lean and obese WT and IL-1RI$^{-/-}$ mice (###P < 0.001 w.r.t. lean; *P < 0.05, ***P < 0.001 w.r.t. WT, n = 9–12). *H*: Body mass composition analysis in lean and obese animals (*P < 0.05 w.r.t. WT obese, n = 8).

rate of weight gain on HFD (Supplementary Fig. 1*D*) and food intake (data not shown) was comparable between strains. Fasting plasma insulin, leptin, triacylglycerol, and nonesterified fatty acids were increased coincident with reduced levels of adiponectin after HFD in both genotypes compared with lean counterparts (Table 1). Plasma IL-6 and TNF-α increased with HFD but was not significantly different between genotypes.

Altered immunogenic phenotype of ATMs from IL-1RI$^{-/-}$ mice despite equivalent macrophage recruitment. Recruitment of macrophages into adipose tissue was monitored to establish potential mechanisms of improved glucose homeostasis in IL-1RI$^{-/-}$ mice. Whereas the number of adipose tissue M1 and M2 macrophages increased with HFD, little difference in recruitment was evident between genotypes (Fig. 2*A* and *B* and

TABLE 1
Plasma metabolic profile

	WT lean	WT obese	IL-1RI$^{-/-}$ lean	IL-1RI$^{-/-}$ obese
Insulin (μg/L)	0.62 ± 0.07	1.66 ± 0.19‡	0.55 ± 0.09	2.90 ± 0.6‖‡
Leptin (ng/mL)	1,091.1 ± 171.2	20,944.3 ± 2,623.8‡	1,152.7 ± 254.5	2,5631.1 ± 1,178.6‡
TNF-α (ng/mL)	16.93 ± 4.88	24.47 ± 4.11	8.42 ± 3.49	28.07 ± 4.69†
IL-6 (ng/mL)	419.1 ± 131.7	1,054.2 ± 188.8	146.4 ± 52.7	1,060.6 ± 214.4*
Nonesterified fatty acid (mmol/L)	1.44 ± 0.19	1.79 ± 0.4	1.29 ± 0.09	2.17 ± 0.17*
Triacylglycerol (mmol/L)	0.75 ± 0.07	1.84 ± 0.41†	1.02 ± 0.18	2.09 ± 0.2*
Adiponectin (ng/mL)	2,733.9 ± 365.4	1,654.1 ± 189.9*	3,084.1 ± 324.4	1,857.1 ± 219.5*

Plasma was isolated from WT and IL-1RI$^{-/-}$ mice by cardiac puncture, and levels of metabolic markers were analyzed enzymatically. *$P <$ 0.05 with respect to (w.r.t.) respective lean. †$P < 0.01$ w.r.t. respective lean. ‡$P < 0.001$ w.r.t. respective lean. ‖$P < 0.01$ w.r.t. WT obese.

Supplementary Fig. 2*C*). Furthermore, there was no difference in the number of T cells or mast cells (Supplementary Fig. 2*A* and *B*). We next monitored cytokine secretion from obese-derived WT and IL-1RI$^{-/-}$ ATMs and demonstrated markedly reduced IL-6 and TNF-α secretion by ATMs from IL-1RI$^{-/-}$ compared with WT mice (Fig. 2*D* and *E*).

Attenuated inflammatory profile of IL-1RI$^{-/-}$ adipose tissue compared with WT ex vivo. We monitored adipose tissue inflammation in explants from lean and obese WT and IL-1RI$^{-/-}$ mice. Secretion of IL-6, TNF-α, and IL-1β was significantly higher from obese adipose explants compared with lean explants (Fig. 3*A*, *C*, and *E*); however, cytokine secretion from IL-1RI$^{-/-}$ explants was significantly reduced compared with WT (Fig. 3*A* and *C*). Furthermore, expression of *IL-6*, *TNF-α*, and *SOCS3* mRNA (Fig. 3*B*, *D*, and *F*) was lower in adipose from IL-1RI$^{-/-}$ mice. HFD-mediated phosphorylation of STAT3 and upregulation of the SOCS3 protein were also attenuated in obese IL-1RI$^{-/-}$ adipose, whereas there was no difference in serine-phosphorylated insulin receptor substrate (IRS)-1 (Fig. 3*G*). Conditioned media from obese adipose explants induced greater activation of NFκB compared with lean explants; nonetheless, obese IL-1RI$^{-/-}$ media had a significantly reduced capacity to drive NFκB compared with WT (Fig. 3*H*).

IL-1RI$^{-/-}$ adipose tissue exhibits greater insulin sensitivity than WT ex vivo. We next sought to establish whether the attenuated inflammatory phenotype of IL-1RI$^{-/-}$ adipose would translate to improved adipose-specific insulin sensitivity. Insulin-stimulated [^{3}H]glucose uptake was significantly higher into adipose of both lean and obese IL-1RI$^{-/-}$ mice compared with WT mice (Fig. 4*A*), coincident with increased insulin-induced tyrosine phosphorylation of IRS-1 (Fig. 4*B*). Expression of phosphorylated AKT was also elevated in lean and obese IL-1RI$^{-/-}$ adipose; however, levels of phosphorylated insulin receptor did not differ between strains (Fig. 4*C* and *D*). Expression of *IRS-1* and *GLUT4* mRNA was significantly higher in lean IL-1RI$^{-/-}$ adipose compared with WT; however, no difference between genotypes was evident after HFD (Fig. 4*E* and *F*). Given this improved insulin-sensitive phenotype of IL-1RI$^{-/-}$ adipose, we further characterized the direct effect of IL-1β on adipocyte biology in vitro. Similar to previous studies (13,14), IL-1β dose-dependently attenuated insulin-stimulated glucose transport into 3T3L1 adipocytes (Supplementary Fig. 3*A*), coincident with downregulation of IRS-1 and GLUT4 mRNA and protein (Supplementary Fig. 3*B* and *C*) and downregulation of peroxisome proliferator–activated receptor (*PPAR*)-γ, sterol regulatory element–binding protein (*SREBP*)-*1c*, perilipin, and fatty acid synthase mRNA (Supplementary Fig. 3*D*). IL-1β also markedly induced IL-6 mRNA and protein secretion from 3T3L1 adipocytes (Supplementary Fig. 3*E* and *F*). IL-6 was also capable of inducing adipocyte IR (Supplementary Fig. 3*G*) (13) and adipocyte lipolysis (28).

Altered adipocyte-macrophage cross-talk between IL-1RI$^{-/-}$ macrophages and 3T3L1 adipocytes. Given the improved insulin-sensitive profile of IL-1RI$^{-/-}$ adipose, we speculated that the reduced immunogenicity of IL-1RI$^{-/-}$ macrophages may result in improved cross-talk with resident adipocytes and preservation of adipocyte functionality. Because the number of ATMs is limited for such mechanistic studies, we determined the effect of IL-1RI$^{-/-}$ versus WT BMMs on adipocyte biology. BMMs from IL-1RI$^{-/-}$ mice had significantly reduced basal expression of *IL-6*, *SOCS3*, and *IL-10* mRNA compared with WT (Fig. 5*H*). Furthermore, IL-1β induced *IL-6*, *SOCS3*, and *IL-10* mRNA expression in WT macrophages but had no effect on IL-1RI$^{-/-}$ BMMs (Supplementary Fig. 4*A–D*). Therefore, IL-1RI$^{-/-}$ BMMs were similarly skewed as the ex vivo ATMs toward a less inflammatory phenotype and thus represented a relevant macrophage phenotype to determine effects on adipocyte biology.

Coculture of WT BMMs with adipocytes significantly reduced insulin-stimulated glucose transport into adipocytes, while coculture with IL-1RI$^{-/-}$ BMM resulted in partial preservation of adipocyte insulin sensitivity (Fig. 5*A* and *B*). Coculture of WT BMMs, but not IL-1RI$^{-/-}$ BMMs, with adipocytes significantly increased IL-6 and TNF-α secretion, with a concomitant reduction in secretion of insulin-sensitizing adiponectin (Fig. 5*C–E*). Furthermore WT, but not IL-1RI$^{-/-}$, BMMs reduced adipocyte *GLUT4*, coincident with increased *IL-6* mRNA expression (Fig. 5*F* and *G*).

Synergy between IL-1 and TNF signaling pathways lost in the absence of IL-1RI. To further probe the mechanisms of attenuated inflammation within IL-1RI$^{-/-}$ adipose and ATMs, we determined the synergistic effect of IL-1β and TNF-α in driving adipocyte/macrophage and adipose tissue inflammation, focusing on IL-6, since this was the most abundant ex vivo adipokine. IL-1β in combination with TNF-α induced greater activation of NFκB than either cytokine alone (Fig. 6*A*). There was marked synergy between IL-1β and TNF-α in promoting IL-6 secretion by adipocytes (Fig. 6*B*). The synergistic effect of IL-1β and TNF-α on IL-6 secretion was ablated in BMM from IL-1RI$^{-/-}$ mice (Fig. 6*C*). TNF-α and IL-1β also synergized to enhance *IL-6*, *IL-1β*, and *SOCS3*, but not *TNF-α*, mRNA expression in WT BMMs (Fig. 6*D–G*), effects that were also abolished in IL-1RI$^{-/-}$ BMMs. We also examined

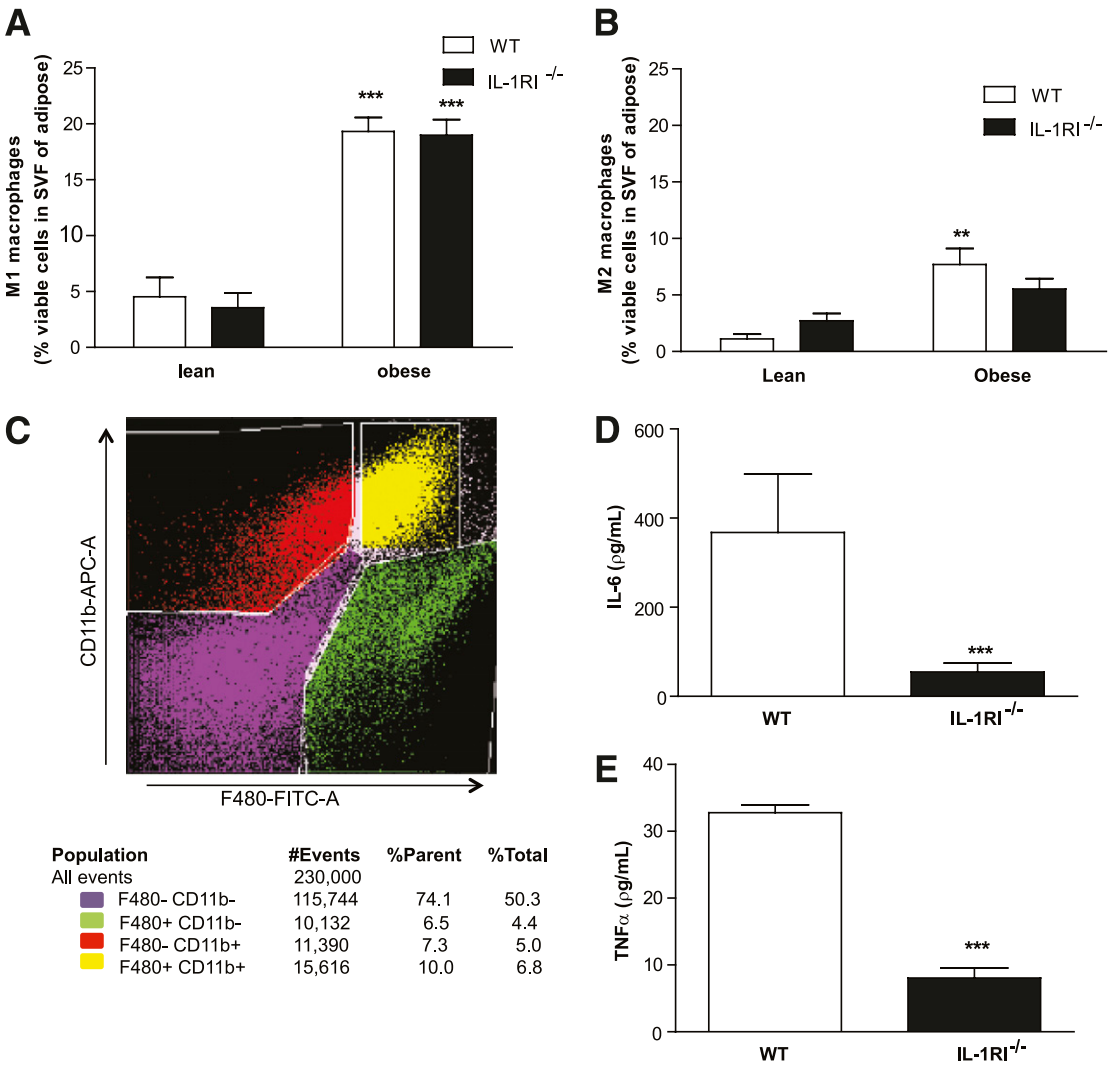

FIG. 2. Recruitment of WT and IL-1RI$^{-/-}$ macrophages into adipose tissue and immunogenic phenotype of isolated ATMs. Adipose tissue was harvested from WT and IL-1RI$^{-/-}$ animals and stromal vascular cells (SVCs) separated from tissue by collagenase digestion. SVCs were labeled with antibodies to F4/80, CD11B, and CD11C and analyzed by flow cytometry. Cells triple positive (F4/80$^+$/CD11B$^+$/CD11C$^+$) were classified as M1 macrophages, whereas cells double positive (F4/80$^+$/CD11B$^+$/CD11C$^-$) were classified as M2 macrophages. Infiltration of M1 (*A*) and M2 (*B*) macrophages into adipose tissue was monitored in lean and obese animals and is presented as percentage of total SVC ($P < 0.01$, ***$P < 0.001$ with respect to [w.r.t.] lean, $n = 10$–30). *C–E*: F4/80$^+$/CD11B$^+$ macrophages were sorted from obese adipose tissue and were seeded in complete media in 24-well plates (200,000 cells/mL media) and left culture for 24 h. Media were harvested and levels of IL-6 (*D*) and TNF-α (*E*) were measured by ELISA (***$P < 0.001$ w.r.t. WT, $n = 6$).**

the effects of IL-1β and TNF-α on adipose IL-6 mRNA expression and protein secretion ex vivo and demonstrated a loss of synergy in IL-1RI$^{-/-}$ explants (Fig. 6*H* and *I*). Furthermore, the ability of TNF-α alone to induce IL-6 was reduced in IL-1RI$^{-/-}$ adipose.

DISCUSSION

Adipose tissue dysfunction due to excessive paracrine inflammation is widely recognized as the earliest and arguably most important step in the etiology of obesity-induced whole-body IR. In the current study, we demonstrate that signaling through the IL-1RI is a key mediator of HFD-induced inflammation in adipose tissue with partial protection of IL-1RI$^{-/-}$ mice from HFD-induced IR.

There have been conflicting findings to date on the role of IL-1 during obesity and in the development of diabetes (36–38), which has been confounded by a central role for IL-1 in regulation of energy homeostasis and weight (37,39). García et al. (37) showed IL-1RI$^{-/-}$ mice maintained on a chow diet develop mature-onset obesity coincident with moderate glucose intolerance and hyperinsulinemia. On the contrary, IL-1Ra$^{-/-}$ mice exhibit a lean phenotype with increased energy expenditure and hypoinsulinemia (39,40). These studies argue for a protective effect of IL-1 against weight gain; however, differences in insulin sensitivity in these mouse models could be solely attributable to differences in weight. In contrast, NOD mice lacking IL-1RI exhibit slower progression but not complete inhibition of diabetes (36), an effect potentially attributable to inhibition of IL-1β–mediated pancreatic β-cell destruction (41,42). Furthermore, and consistent with our findings, treatment of HFD-fed mice with IL-1Ra improved glucose homeostasis and enhanced insulin secretion, with protection of β-cells from HFD-mediated toxicity (38). However, the effect of IL-1Ra on

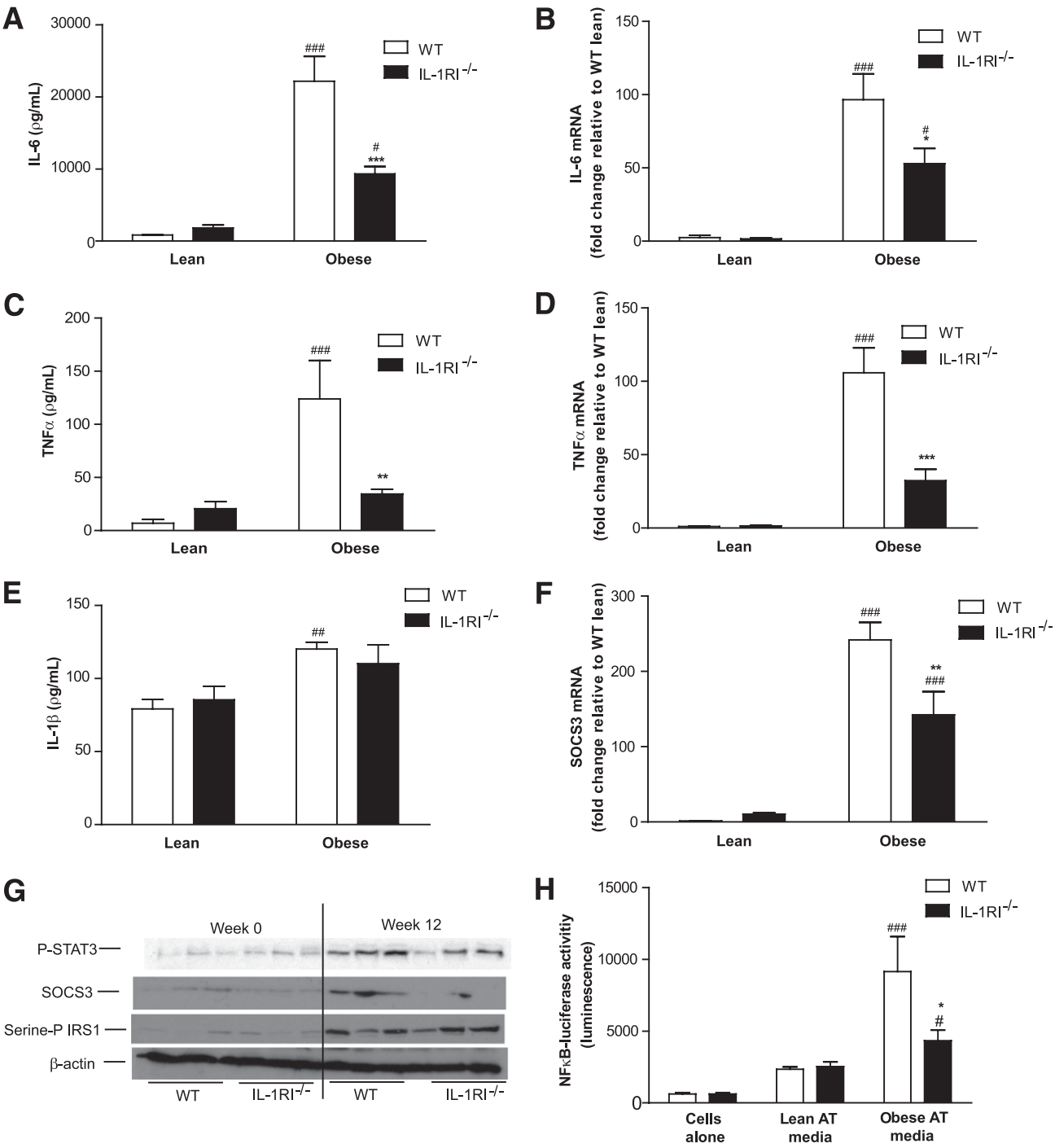

FIG. 3. Inflammatory signature of WT and IL-1RI$^{-/-}$ adipose. Adipose explants were cultured for 24 h in serum-containing media (100 mg/mL media) and levels of proinflammatory IL-6 (*A*), TNF-α (*C*), and IL-1β secretion into media (*E*) were measured by ELISA (*$P < 0.05$, **$P < 0.01$, ***$P < 0.001$ with respect to [w.r.t.] WT; #$P < 0.05$, ##$P < 0.01$, ###$P < 0.001$ w.r.t. corresponding lean, $n = 8$–12). Adipose tissue mRNA levels of IL-6 (*B*), TNF-α (*D*), and SOCS3 (*F*) were analyzed by real-time PCR (*$P < 0.5$, **$P < 0.01$, ***$P < 0.001$ w.r.t. WT; #$P < 0.05$, ###$P < 0.001$ w.r.t. lean, $n = 8$). *G*: WT and IL-1RI$^{-/-}$ adipose tissue protein lysates at weeks 0 and 12 post-HFD were probed for levels of phosphorylated STAT3, SOCS3, serine-phosphorylated IRS-1, and β-actin by immunoblot analysis. *H*: Adipose-tissue conditioned media were applied for 6 h to NIH-3T3 cells stably expressing an NFκB-luciferase promoter-reporter construct to monitor NFκB activity. Levels of NFκB-driven luciferase were quantified using a luminometer (*$P < 0.05$ w.r.t. corresponding WT; #$P < 0.05$, ###$P < 0.001$ w.r.t. lean AT media, $n = 8$).

adipose tissue biology and insulin sensitivity was not assessed. Recent human trials have shown that treatment with IL-1Ra (anakinra) improves glycemia and β-cell secretory function, coincident with reduced systemic inflammation in patients with type 2 diabetes (43). This trial did not demonstrate improved insulin sensitivity after 13 weeks. Intervention in high-risk prediabetic obese cohorts may yield more promising results, wherein IL-1RI inhibition may delay, if not prevent, development of type 2 diabetes by attenuating adipose inflammation and protecting functional β-cells. Our study adds insight into the potential initial contribution of IL-1RI signaling during

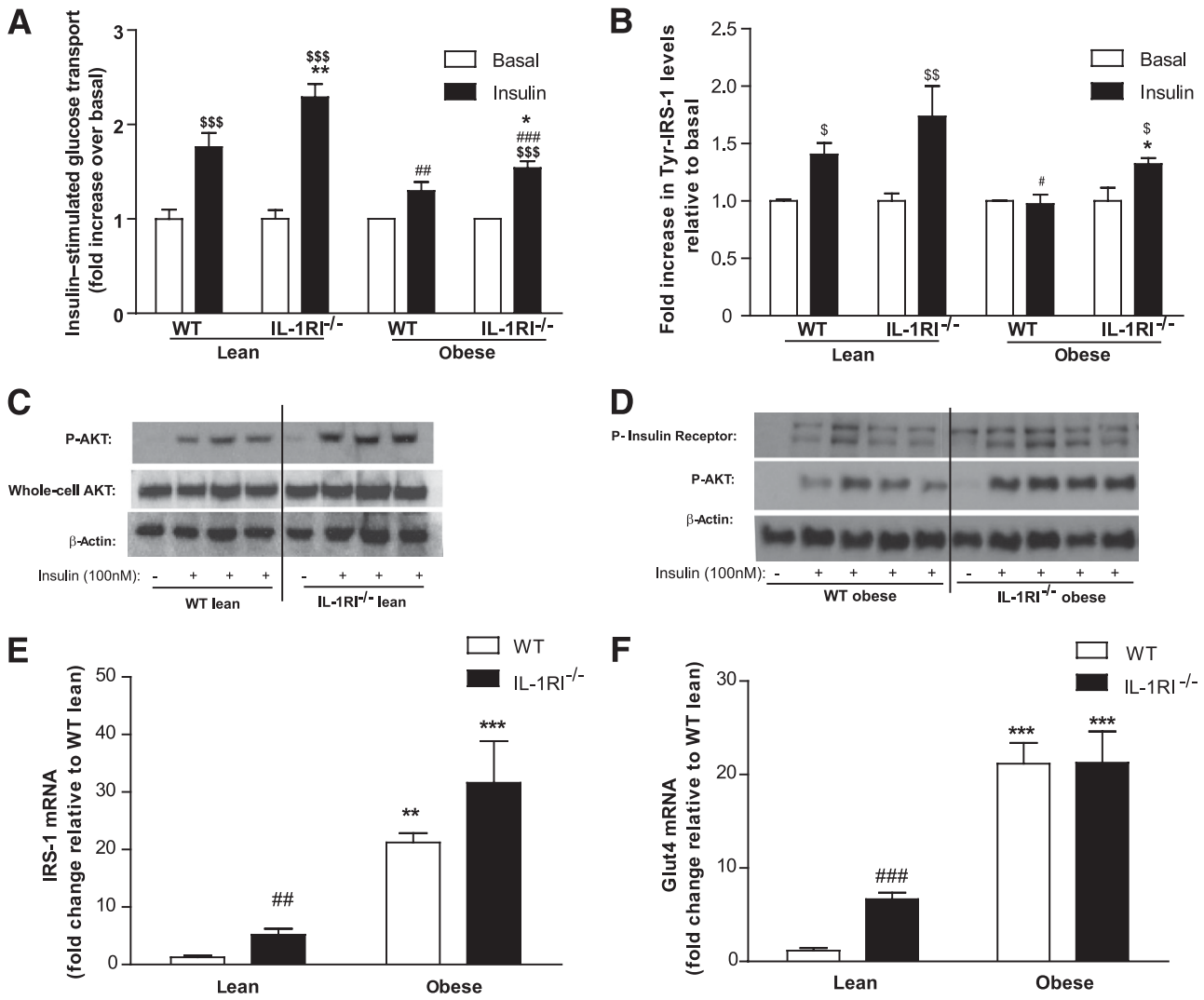

FIG. 4. Ex vivo evaluation of adipose tissue insulin sensitivity. *A*: Adipose explants from lean and obese WT and IL-1RI$^{-/-}$ mice were harvested and stimulated ± insulin (100 nmol/L) ex vivo for 15 min. Tracer [^{3}H]glucose was added to explants for an additional 45 min. Levels of [^{3}H]glucose were measured by liquid scintillation counting. Fold increase in [^{3}H]glucose transport in response to insulin over basal (non–insulin-stimulated) into adipose tissue for each individual mouse was calculated and is presented (##*P* < 0.01, ###*P* < 0.001 w.r.t. lean; **P* < 0.05, ***P* < 0.01 with respect to [w.r.t.] WT; $$$*P* < 0.001 w.r.t. basal, *n* = 8). *B–D*: Protein lysates were prepared from adipose tissue of lean and obese WT and IL-1RI$^{-/-}$ mice after stimulation ± insulin (100 nmol/L) for 1 h ex vivo. *A*: Levels of tyrosine phosphorylated IRS-1 in adipose protein lysates were measured using a PathScan ELISA kit (#*P* < 0.05 w.r.t. WT lean; **P* < 0.05 w.r.t. WT obese; $*P* < 0.05, $$*P* < 0.01 w.r.t. basal, *n* = 8). Levels of phosphorylated AKT, phosphorylated insulin receptor, whole-cell AKT, and β-actin in lean (*C*) and obese (*D*) adipose protein lysates were assessed by immunoblot analysis. Adipose tissue mRNA levels of IRS-1 (*E*) and GLUT4 (*F*) were analyzed by real-time PCR analysis (*P* < 0.01, ****P* < 0.001 w.r.t. lean; ##*P* < 0.01, ###*P* < 0.001 w.r.t. WT, *n* = 8).**

early phases of obesity-induced IR, particularly in adipose tissue.

Our in vivo findings demonstrate that lack of IL-1RI partially protects mice from HFD-induced IR, with improved glucose homeostasis and enhanced insulin sensitivity observed in obese IL-1RI$^{-/-}$ compared with WT mice. Plasma concentrations of triacylglycerol, nonesterified fatty acid, IL-6, and TNF-α did not differ between strains; however, consistent with a previous report (37), levels of insulin were elevated in obese IL-1RI$^{-/-}$ mice. This hyperinsulinemia was not associated with IR and appears to be an intrinsic characteristic of the animal model given the converse hypoinsulinemic phenotype of IL-1Ra$^{-/-}$ mice (39). Prediet lean IL-1RI$^{-/-}$ mice cleared glucose more efficiently than WT during GTT, which may be attributable to enhanced insulin secretion in response to glucose load, together with heightened adipose tissue insulin sensitivity. This phenotype was age-dependent; glucose tolerance was equivalent in older chow-fed IL-1RI$^{-/-}$ and WT mice, coincident with enhanced weight gain in the IL-1RI$^{-/-}$ mice as previously reported (37). Interestingly, HFD-fed IL-1RI$^{-/-}$ mice did not develop further IR compared with age-matched chow-fed IL-1RI$^{-/-}$ mice, despite much greater weight gain, providing further evidence of protection against HFD-induced IR but not obesity.

Immune cell recruitment into adipose plays a key role in the etiology of HFD-induced IR (6), prompting us to speculate that reduced immune cell number in IL-1RI$^{-/-}$ adipose may partially account for improved glucose homeostasis. Contrary to our hypothesis, the number of tissue M1/M2 in adipose was not different between IL-1RI$^{-/-}$ and WT mice after HFD, demonstrating little role for IL-1 in immune cell chemotaxis. We next speculated the cytokine signature of ATMs may be altered in IL-1RI$^{-/-}$ mice.

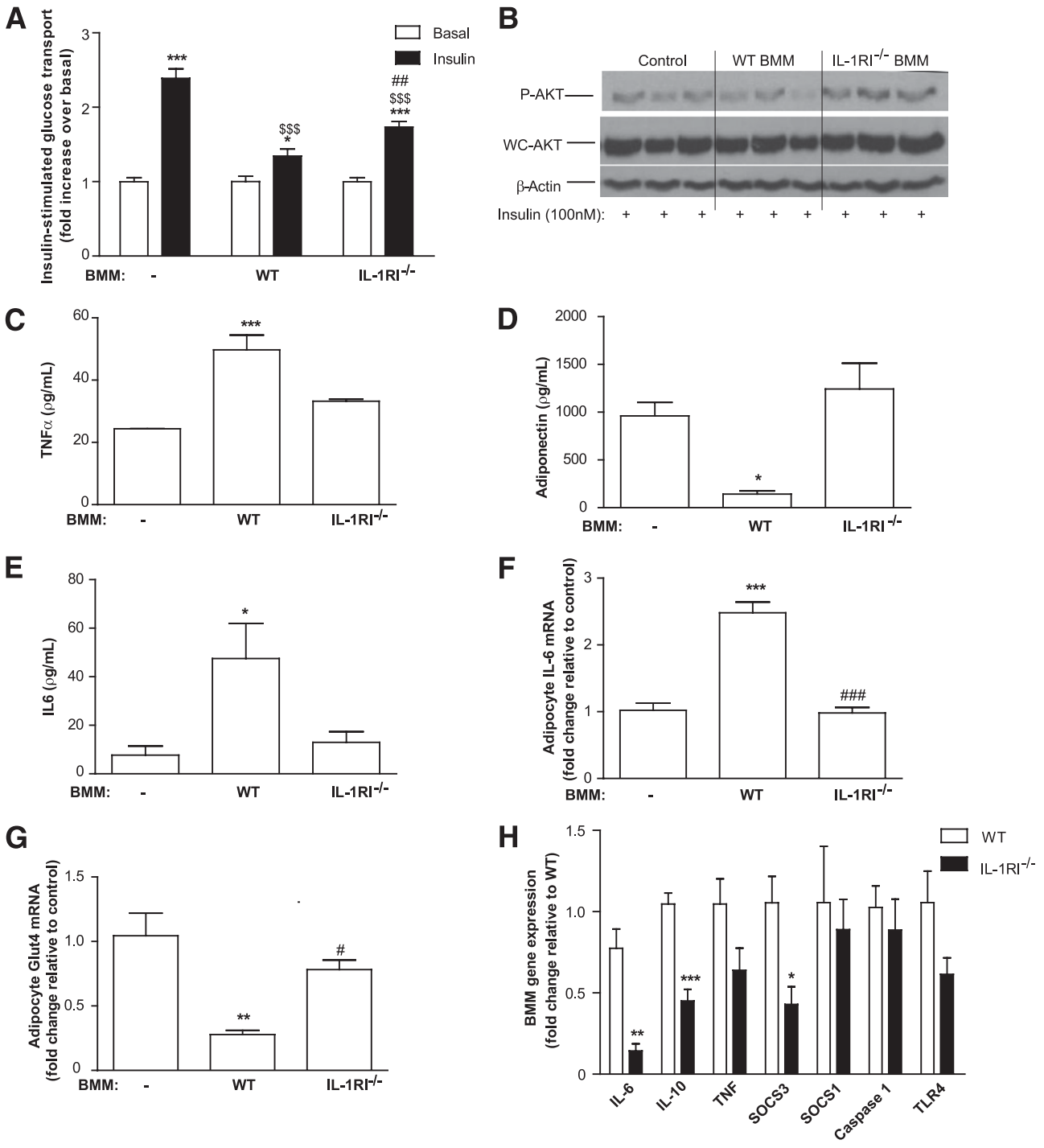

FIG. 5. Cross-talk of WT and IL-1RI$^{-/-}$ BMMs with 3T3L1 adipocytes. WT and IL-1RI$^{-/-}$ BMMs, seeded on transwell (0.4 μmol/L thickness) inserts, were stimulated with LPS (100 ng/mL) for 30 min, washed with PBS before addition of fresh media, and transferred to 3T3L1 adipocyte plates where cells were left to coculture for 5 days. *A*: The effect of BMMs on insulin (100 nmol/L)-stimulated [^{3}H]glucose transport into 3T3L1 adipocytes was evaluated. Fold increase in [^{3}H]glucose transport into adipocytes in response to insulin over basal (non-insulin–stimulated) is presented (P* < 0.05, ****P* < 0.001 with respect to [w.r.t.] individual basal; $$$*P* < 0.001 w.r.t. control + insulin; ##*P* < 0.01 w.r.t. WT BMM + insulin, *n* = 4). *B*: Protein lysates from cocultured adipocytes stimulated with insulin (100 nmol/L) for 15 min were harvested and probed for levels of phosphorylated AKT, whole-cell AKT, and β-actin by immunoblot analysis. *C–E*: Media from cocultured cells were harvested after 72 h and levels of TNF-α (*C*), adiponectin (*D*), and IL-6 (*E*) were measured by ELISA (**P* < 0.05, ****P* < 0.001 w.r.t. adipocytes alone, *n* = 4). *F* and *G*: Effect of coculture with WT or IL-1RI$^{-/-}$ BMMs on adipocyte IL-6 (*F*) and Glut4 (*G*) mRNA expression by real-time PCR (***P* < 0.01, ****P* < 0.001 w.r.t. control; #*P* < 0.05, ###*P* < 0.001 w.r.t. IL-1RI$^{-/-}$ coculture, *n* = 4). *H*: Baseline inflammatory mRNA signature of WT and IL-1RI$^{-/-}$ BMMs. Basal mRNA levels of IL-6, IL-10, TNF-α, SOCS3, SOCS1, caspase 1, and TLR4 in WT and IL-1RI$^{-/-}$ BMMs as assessed by real-time PCR (**P* < 0.05, ***P* < 0.01, ****P* < 0.001 w.r.t. WT, *n* = 4).**

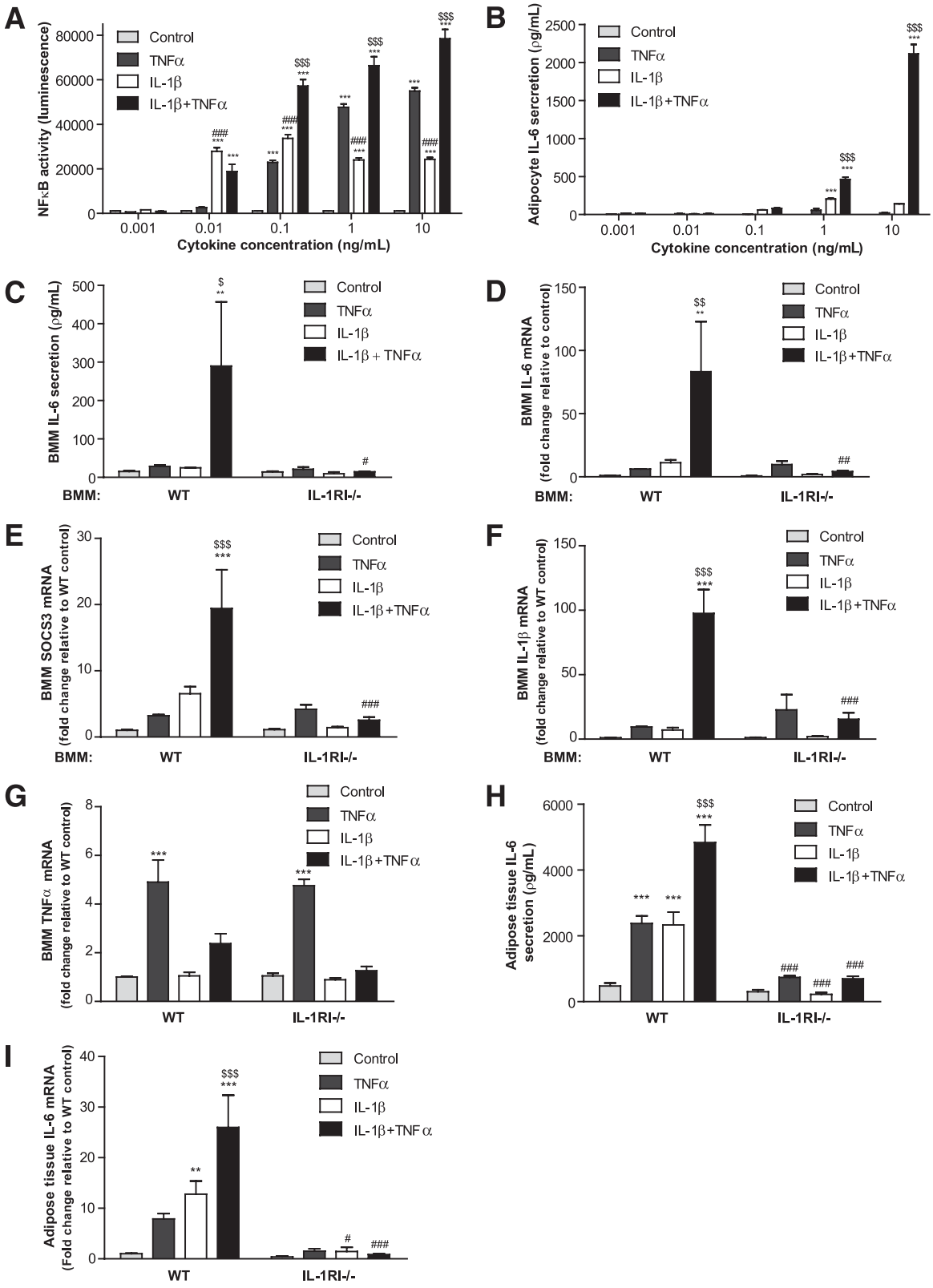

FIG. 6. IL-1β and TNF-α synergize to enhance adipose tissue inflammation and NFκB activity. *A*: NIH-3T3 cells stably expressing an NFκB-luciferase promoter-reporter construct were treated with increasing concentrations of IL-1β or TNF-α alone or both in combination for 6 h. Levels of NFκB-driven luciferase were quantified using a luminometer (*$P < 0.001$ with respect to [w.r.t.] control; ###$P < 0.001$ w.r.t. TNF alone; $$$$P < 0.001$ w.r.t. either cytokine alone, $n = 4$). *B*: 3T3L1 adipocytes were treated ± IL-1β ± TNF-α for 24 h, and levels of IL-6 secreted were measured by ELISA (***$P < 0.001$ w.r.t. control; $$$$P < 0.001$ w.r.t. either cytokine alone, $n = 4$). *C–G*: BMMs were harvested from WT and IL-1RI$^{-/-}$ mice and stimulated ± IL-1β ± TNF-α (10 ng/mL) for 24 h, and levels of IL-6 (*C*) secreted measured by ELISA and IL-6 (*D*), SOCS3 (*E*), IL-1β (*F*), and TNFα mRNA (*G*) were measured by real-time PCR (**$P < 0.01$, ***$P < 0.001$ w.r.t. control; #$P < 0.05$, ##$P < 0.01$, ###$P < 0.001$ w.r.t. WT; $$P < 0.05$, $$$P < 0.01$, $$$$P < 0.001$ w.r.t. either cytokine alone, $n = 3$). *H* and *I*: Adipose tissue explants (100 mg) were harvested from lean WT and IL-1RI$^{-/-}$ mice and were cultured for 6 h ± IL-1β ± TNF-α (10 ng/mL) and levels of IL-6 secretion (*H*) and IL-6 mRNA (*I*) were determined (***$P < 0.001$ w.r.t. control; #$P < 0.05$, ###$P < 0.001$ w.r.t. WT; $$$$P < 0.001$ w.r.t. either cytokine alone, $n = 5$).**

Robust cytokine secretion from WT ATMs was evident after 24 h in culture in the absence of any external stimulus, indicative of preactivation within the inflamed environment of the obese tissue before culture ex vivo. By contrast, cytokine secretion from IL-1RI$^{-/-}$ ATMs was markedly lower, suggestive of altered immunogenicity. A recent report demonstrated removal of HFD from WT obese animals improved insulin sensitivity before reduction in macrophage number; however, the proinflammatory phenotype of these ATMs was markedly attenuated upon removal of HFD, demonstrating phenotypic plasticity (44). It is therefore arguable that it is not the number of macrophages per se that determine poor outcome, but the activation state, cytokine signature, and functional effects of ATMs that dictate severity of IR. Upon culture, IL-1RI$^{-/-}$ ATMs secreted markedly reduced levels of both TNF-α and IL-6, and it is thus likely that altered immunogenic phenotype of recruited IL-1RI$^{-/-}$ immune cells results in improved cross-talk with resident adipocytes and improved insulin sensitivity. Consistent with this, we demonstrated improved cytokine cross-talk of IL-1RI$^{-/-}$ BMMs with 3T3L1 adipocytes in vitro, coincident with an attenuated effect on adipocyte insulin sensitivity compared with WT BMMs.

Given the prominent role for adipose tissue dysfunction in early stages of obesity-induced IR and the attenuated immunogenic profile of IL-1RI$^{-/-}$ ATMs, we next hypothesized that IL-1RI–transduced signals may contribute to HFD-induced inflammation within whole adipose tissue. Previous findings in our laboratory highlighted attenuated inflammatory and cellular stress–related proteomic signature exclusive to adipose tissue rather than skeletal muscle or liver in obese IL-1RI$^{-/-}$ mice compared with WT mice (45). The present work extends our understanding of the paracrine effect associated with lack of IL-1RI in adipose tissue with reduced IL-6 and TNF-α secretion from explants coincident with reduced mRNA expression of *TNF-α*, *IL-6*, and *SOCS3*. Furthermore, we demonstrate reduced activation of STAT3 coincident with reduced SOCS3 protein in IL-1RI$^{-/-}$ adipose, an effect potentially attributable to reduced IL-6 secretion. This effect reduced local adipose tissue inflammation in turn correlated with improved insulin sensitivity of IL-1RI$^{-/-}$ adipose ex vivo. Interestingly, this attenuated inflammatory profile was localized to adipose tissue with equivalent concentrations of systemic cytokines in IL-1RI$^{-/-}$ and WT mice. The discrepancy between systemic and local cytokine levels is unclear, but may be attributable to almost undetectable plasma IL-1β levels in WT animals, even with obesity (46,47), compared with the concentration of IL-1β in macrophages/adipose tissue.

Whereas IL-1RI signaling clearly plays a nonredundant role during HFD-induced IR, it may be an oversimplification to attribute the majority of adipose tissue inflammation to the actions of one cytokine. It is much more likely that adipose-derived cytokines cross-talk to amplify adipose tissue inflammation. Consistent with this hypothesis, we demonstrated a potent synergistic effect of the major adipocytokines IL-1β and TNF-α in enhancing NFκB activation and adipose IL-6 protein secretion. This synergistic effect on macrophage and adipose IL-6 secretion was lost in the absence of IL-1RI. Furthermore, the ability of TNF-α to induce IL-6 secretion was blunted in IL-1RI$^{-/-}$ adipose, suggesting that TNF-α–induced IL-6 is in part mediated via IL-1. Remarkably, TNF-α and IL-1β synergized to enhance *IL-1β* mRNA expression in WT BMMs far beyond the effects of either cytokine alone, suggesting that these cytokines work in concert to create a positive feedback loop. Interestingly, *TNF-α* mRNA expression was not enhanced, suggesting differential regulatory mechanisms for *TNF-α* mRNA. These findings suggest that blocking IL-1 signaling not only ameliorates the adverse effects of IL-1 on adipocyte/macrophage biology, but also prevents the synergy between TNF-α and IL-1β, thus alleviating adipose tissue inflammation.

Recent reports demonstrating activation of the NLRP3 inflammasome following an HFD and protection of inflammasome-compromised mice against HFD-induced IR (19,20) have given new insight into the upstream mechanisms through which IL-1 is elevated during obesity. We have focused on the downstream consequences of IL-1RI signaling within adipose tissue during an HFD and have demonstrated that IL-1RI$^{-/-}$ mice are protected against HFD-induced IR coincident with attenuated adipose tissue and ATM inflammation. There are numerous local cellular targets and functional consequences of IL-1 released from adipose tissue, including preadipocytes (inhibition of adipogenesis), mature adipocytes (induction of IR), and infiltrated immune cells (enhanced cytokine secretion), all of which may contribute to adipose tissue IR. However, our study is limited in its ability to distinguish whether lack of IL-1RI signaling in immune cells or in adipocyte/preadipocyte fractions is primarily responsible for this improved phenotype. Metabolic studies in animals with either immune-specific or adipocyte-specific deletion of IL-1RI would in turn provide greater insight into these mechanistic queries.

In conclusion, we ascribe a pathogenic role to IL-1RI–mediated signals during HFD-induced adipose tissue dysfunction and IR. Improved glucose homeostasis in IL-1RI$^{-/-}$ mice correlated with a marked reduction in local adipose inflammation, with altered ATM cytokine signatures and pronounced attenuation in both IL-6 secretion and activation of the IL-6 regulated proteins STAT3 and SOCS3. Loss of synergy between TNF-α and IL-1β in IL-1RI$^{-/-}$ adipose may in turn have contributed to this attenuated inflammatory profile. This study highlights the critical and nonredundant contribution of IL-1 to the medley of proinflammatory insulin-desensitizing signals relevant to obesity-induced IR.

ACKNOWLEDGMENTS

This work was supported by the Science Foundation Ireland PI Programme (06/IM.1/B105) (to H.M.R.).

No potential conflicts of interest relevant to this article were reported.

F.C.M. researched data and wrote the manuscript. K.A.H. and C.M.R. researched data and proofread the manuscript. E.O. and M.C. researched data. K.H.G.M. reviewed data and edited the manuscript. H.M.R. designed the study, reviewed data, and edited the manuscript.

The authors appreciate the technical support from the core technologies staff in the Conway Institute, University College Dublin, Belfield, Dublin, Ireland, and the technical support of Dr. Eileen Murphy during body composition analysis in the Alimentary Pharmabiotic Center, University College Cork, Cork, Ireland.

REFERENCES

1. Winer S, Chan Y, Paltser G, et al. Normalization of obesity-associated insulin resistance through immunotherapy. Nat Med 2009;15:921–929
2. Nishimura S, Manabe I, Nagasaki M, et al. CD8+ effector T cells contribute to macrophage recruitment and adipose tissue inflammation in obesity. Nat Med 2009;15:914–920

3. Kintscher U, Hartge M, Hess K, et al. T-lymphocyte infiltration in visceral adipose tissue: a primary event in adipose tissue inflammation and the development of obesity-mediated insulin resistance. Arterioscler Thromb Vasc Biol 2008;28:1304–1310
4. Rausch ME, Weisberg S, Vardhana P, Tortoriello DV. Obesity in C57BL/6J mice is characterized by adipose tissue hypoxia and cytotoxic T-cell infiltration. Int J Obes (Lond) 2008;32:451–463
5. Lumeng CN, Deyoung SM, Bodzin JL, Saltiel AR. Increased inflammatory properties of adipose tissue macrophages recruited during diet-induced obesity. Diabetes 2007;56:16–23
6. Weisberg SP, McCann D, Desai M, Rosenbaum M, Leibel RL, Ferrante AW Jr. Obesity is associated with macrophage accumulation in adipose tissue. J Clin Invest 2003;112:1796–1808
7. Shoelson SE, Lee J, Goldfine AB. Inflammation and insulin resistance. J Clin Invest 2006;116:1793–1801
8. Kern PA, Saghizadeh M, Ong JM, Bosch RJ, Deem R, Simsolo RB. The expression of tumor necrosis factor in human adipose tissue. Regulation by obesity, weight loss, and relationship to lipoprotein lipase. J Clin Invest 1995;95:2111–2119
9. Fenkci S, Rota S, Sabir N, Sermez Y, Guclu A, Akdag B. Relationship of serum interleukin-6 and tumor necrosis factor alpha levels with abdominal fat distribution evaluated by ultrasonography in overweight or obese postmenopausal women. J Investig Med 2006;54:455–460
10. Wellen KE, Hotamisligil GS. Inflammation, stress, and diabetes. J Clin Invest 2005;115:1111–1119
11. Nov O, Kohl A, Lewis EC, et al. Interleukin-1β may mediate insulin resistance in liver-derived cells in response to adipocyte inflammation. Endocrinology 2010;151:4247–4256
12. Hotamisligil GS, Murray DL, Choy LN, Spiegelman BM. Tumor necrosis factor alpha inhibits signaling from the insulin receptor. Proc Natl Acad Sci U S A 1994;91:4854–4858
13. Tanaka T, Itoh H, Doi K, et al. Down regulation of peroxisome proliferator-activated receptorgamma expression by inflammatory cytokines and its reversal by thiazolidinediones. Diabetologia 1999;42:702–710
14. Jager J, Grémeaux T, Cormont M, Le Marchand-Brustel Y, Tanti JF. Interleukin-1beta-induced insulin resistance in adipocytes through down-regulation of insulin receptor substrate-1 expression. Endocrinology 2007;148:241–251
15. Uysal KT, Wiesbrock SM, Marino MW, Hotamisligil GS. Protection from obesity-induced insulin resistance in mice lacking TNF-alpha function. Nature 1997;389:610–614
16. Poggi M, Bastelica D, Gual P, et al. C3H/HeJ mice carrying a toll-like receptor 4 mutation are protected against the development of insulin resistance in white adipose tissue in response to a high-fat diet. Diabetologia 2007;50:1267–1276
17. Shi H, Kokoeva MV, Inouye K, Tzameli I, Yin H, Flier JS. TLR4 links innate immunity and fatty acid-induced insulin resistance. J Clin Invest 2006;116:3015–3025
18. Mills KH, Dunne A. Immune modulation: IL-1, master mediator or initiator of inflammation. Nat Med 2009;15:1363–1364
19. Vandanmagsar B, Youm YH, Ravussin A, et al. The NLRP3 inflammasome instigates obesity-induced inflammation and insulin resistance. Nat Med 2011;17:179–188
20. Stienstra R, Joosten LA, Koenen T, et al. The inflammasome-mediated caspase-1 activation controls adipocyte differentiation and insulin sensitivity. Cell Metab 2010;12:593–605
21. Maedler K, Dharmadhikari G, Schumann DM, Størling J. Interleukin-1 beta targeted therapy for type 2 diabetes. Expert Opin Biol Ther 2009;9:1177–1188
22. Stylianou E, Saklatvala J. Interleukin-1. Int J Biochem Cell Biol 1998;30:1075–1079
23. Hirosumi J, Tuncman G, Chang L, et al. A central role for JNK in obesity and insulin resistance. Nature 2002;420:333–336
24. Shoelson SE, Lee J, Yuan M. Inflammation and the IKK beta/I kappa B/NF-kappa B axis in obesity- and diet-induced insulin resistance. Int J Obes Relat Metab Disord 2003;27(Suppl. 3):S49–S52
25. Verstrepen L, Bekaert T, Chau TL, Tavernier J, Chariot A, Beyaert R. TLR-4, IL-1R and TNF-R signaling to NF-kappaB: variations on a common theme. Cell Mol Life Sci 2008;65:2964–2978
26. Arkan MC, Hevener AL, Greten FR, et al. IKK-beta links inflammation to obesity-induced insulin resistance. Nat Med 2005;11:191–198
27. Yuan M, Konstantopoulos N, Lee J, et al. Reversal of obesity- and diet-induced insulin resistance with salicylates or targeted disruption of Ikk-beta. Science 2001;293:1673–1677
28. Yang Y, Ju D, Zhang M, Yang G. Interleukin-6 stimulates lipolysis in porcine adipocytes. Endocrine 2008;33:261–269
29. Lagathu C, Yvan-Charvet L, Bastard JP, et al. Long-term treatment with interleukin-1beta induces insulin resistance in murine and human adipocytes. Diabetologia 2006;49:2162–2173
30. Emanuelli B, Peraldi P, Filloux C, et al. SOCS-3 inhibits insulin signaling and is up-regulated in response to tumor necrosis factor-alpha in the adipose tissue of obese mice. J Biol Chem 2001;276:47944–47949
31. Ueki K, Kondo T, Kahn CR. Suppressor of cytokine signaling 1 (SOCS-1) and SOCS-3 cause insulin resistance through inhibition of tyrosine phosphorylation of insulin receptor substrate proteins by discrete mechanisms. Mol Cell Biol 2004;24:5434–5446
32. Niemand C, Nimmesgern A, Haan S, et al. Activation of STAT3 by IL-6 and IL-10 in primary human macrophages is differentially modulated by suppressor of cytokine signaling 3. J Immunol 2003;170:3263–3272
33. Elmendorf JS, Chen D, Pessin JE. Guanosine 5′-O-(3-thiotriphosphate) (GTPgammaS) stimulation of GLUT4 translocation is tyrosine kinase-dependent. J Biol Chem 1998;273:13289–13296
34. Wang X, Collins HL, Ranalletta M, et al. Macrophage ABCA1 and ABCG1, but not SR-BI, promote macrophage reverse cholesterol transport in vivo. J Clin Invest 2007;117:2216–2224
35. McGillicuddy FC, Chiquoine EH, Hinkle CC, et al. Interferon gamma attenuates insulin signaling, lipid storage, and differentiation in human adipocytes via activation of the JAK/STAT pathway. J Biol Chem 2009;284:31936–31944
36. Thomas HE, Irawaty W, Darwiche R, et al. IL-1 receptor deficiency slows progression to diabetes in the NOD mouse. Diabetes 2004;53:113–121
37. García MC, Wernstedt I, Berndtsson A, et al. Mature-onset obesity in interleukin-1 receptor I knockout mice. Diabetes 2006;55:1205–1213
38. Sauter NS, Schulthess FT, Galasso R, Castellani LW, Maedler K. The anti-inflammatory cytokine interleukin-1 receptor antagonist protects from high-fat diet-induced hyperglycemia. Endocrinology 2008;149:2208–2218
39. Somm E, Henrichot E, Pernin A, et al. Decreased fat mass in interleukin-1 receptor antagonist-deficient mice: impact on adipogenesis, food intake, and energy expenditure. Diabetes 2005;54:3503–3509
40. Matsuki T, Horai R, Sudo K, Iwakura Y. IL-1 plays an important role in lipid metabolism by regulating insulin levels under physiological conditions. J Exp Med 2003;198:877–888
41. Bendtzen K, Mandrup-Poulsen T, Nerup J, Nielsen JH, Dinarello CA, Svenson M. Cytotoxicity of human pI 7 interleukin-1 for pancreatic islets of Langerhans. Science 1986;232:1545–1547
42. Maedler K, Sergeev P, Ris F, et al. Glucose-induced beta cell production of IL-1beta contributes to glucotoxicity in human pancreatic islets. J Clin Invest 2002;110:851–860
43. Larsen CM, Faulenbach M, Vaag A, et al. Interleukin-1-receptor antagonist in type 2 diabetes mellitus. N Engl J Med 2007;356:1517–1526
44. Li P, Lu M, Nguyen MT, et al. Functional heterogeneity of CD11c-positive adipose tissue macrophages in diet-induced obese mice. J Biol Chem 2010;285:15333–15345
45. de Roos B, Rungapamestry V, Ross K, et al. Attenuation of inflammation and cellular stress-related pathways maintains insulin sensitivity in obese type I interleukin-1 receptor knockout mice on a high-fat diet. Proteomics 2009;9:3244–3256
46. Jung C, Gerdes N, Fritzenwanger M, Figulla HR. Circulating levels of interleukin-1 family cytokines in overweight adolescents. Mediators Inflamm 2010;2010:958403
47. van der Poll T, Marchant A, Buurman WA, et al. Endogenous IL-10 protects mice from death during septic peritonitis. J Immunol 1995;155:5397–5401